Electron properties of high-speed solar wind from polar coronal holes obtained by Ulysses thermal noise spectroscopy: Not so dense, not so hot

K. Issautier,[1] G. Le Chat,[1] N. Meyer-Vernet,[1] M. Moncuquet,[1] S. Hoang,[1] R. J. MacDowall,[2] and D. J. McComas[3]

Received 4 June 2008; revised 1 August 2008; accepted 7 August 2008; published 1 October 2008.

[1] We present radio observations of Ulysses' third fast latitude scan near the 2007 solar activity minimum of cycle 23. We deduce in situ measurements of the electron density and temperature using the method of quasi-thermal noise spectroscopy. We study the large-scale properties of the fast solar wind coming from polar coronal holes and compare our results to those obtained during Ulysses' first fast scan in 1994–1995 near the minimum of cycle 22. The fast solar wind in both hemispheres is less dense and cooler by about 19% and 13% respectively, as compared to the last solar minimum. **Citation:** Issautier, K., G. Le Chat, N. Meyer-Vernet, M. Moncuquet, S. Hoang, R. J. MacDowall, and D. J. McComas (2008), Electron properties of high-speed solar wind from polar coronal holes obtained by Ulysses thermal noise spectroscopy: Not so dense, not so hot, *Geophys. Res. Lett.*, *35*, L19101, doi:10.1029/2008GL034912.

1. Introduction

[2] After more than 17 years in the heliosphere, Ulysses has given another picture of the solar wind during its third orbit around the Sun. Launched in 1990, Ulysses is the only spacecraft exploring the three dimensional structure of the heliosphere through the solar cycle. The first pole-to-pole fast transit occurred in 1994–1995 near the minimum of solar cycle 22, when Ulysses explored the heliographic latitudes from 80°S to 80°N. This offered the opportunity to study the radial and latitudinal structure of the solar wind with minimal variation in the phase of the solar activity cycle since the passage lasts only about 10 months. Ulysses confirmed the rather simple structure of the corona during solar minimum and showed that two kinds of wind dominate the heliosphere. A steady-state fast wind was continuously observed at high latitudes, coming from large polar coronal holes, whereas within 20°S and N a rather complex mixture of winds predominated in the solar equator [*Phillips et al.*, 1995; *McComas et al.*, 2000; *Issautier et al.*, 1998; *Neugebauer*, 2001]. In contrast, during the rising phase of solar activity 22 to the 2001 maximum, Ulysses showed a dramatically different corona, and a complex solar wind structure with different regimes, slow and intermediate wind from streamers, flow interactions, in addition to sporadic fast flows from small coronal holes at all heliolatitudes [*Luhmann et al.*, 2002; *McComas et al.*, 2003; *Smith et al.*, 2003; *Issautier et al.*, 2004]. During the 2001 maximum, a long interval of fast wind coming from a polar coronal hole was however observed at high northern latitudes above 72°N [*McComas et al.*, 2002]. During that period, among other parameters, the electron density and temperature were found to be similar to those observed in polar coronal holes in 1994–1995, near solar minimum, suggesting that the properties of the fast wind from polar coronal holes could be independent of the phase of the solar cycle [*von Steiger et al.*, 2001; *McComas et al.*, 2003; *Issautier et al.*, 2003, 2004]. Since February 2007, Ulysses undertook a third pole-to-pole fast transit, near the minimum of cycle 23 when the solar magnetic dipole reversed with respect to the previous minimum [*Smith et al.*, 2003]. In this paper, we study the large-scale electron properties obtained during the 2007 fast latitude scan using data from the Unified Radio and Plasma wave (URAP) instrument [*Stone et al.*, 1992]. We concentrate on the fast solar wind associated with polar coronal holes and compare it with the results obtained during the two previous fast transits, thereby spanning a complete solar cycle. The data were obtained from the URAP radio receiver from 1 May to 26 November 2007, over a latitudinal range of 60°S to 68°N, and at radial distance ranging from 1.8 AU at 60°S and 1.76 AU at 68°N, to 1.4 AU at perihelion. Due to spacecraft power limitations and energy sharing, the URAP experiment was turned off during the highest latitude passages in both the southern (poleward 60°) and northern (poleward 68°) hemispheres.

2. Basics of in Situ Diagnostics With Quasi-Thermal Noise Spectroscopy

[3] In situ electron measurements are performed by the low-band radio receiver of the URAP experiment. This receiver is connected to the 2 × 35-m thin strip dipole antenna and covers the frequency range from 1.25 to 48.5 kHz in 128 s. We derive electron macroscopic parameters using quasi-thermal noise (QTN) spectroscopy. This technique consists in measuring the electrostatic fluctuations produced at the antenna ports by the quasi-thermal motion of the ambient electrons and protons [*Meyer-Vernet et al.*, 1998, and references therein]. The theoretical spectrum is a function of the velocity distribution of the particles for which we assume a sum of two Maxwellians for electrons, with a core (density N_c, temperature T_c) and a halo (density N_h, temperature T_h), and one drifting Maxwellian for protons (temperature T_p, speed V) [*Issautier et al.*,

[1]Laboratoire d'Etudes Spatiales et d'Instrumentation en Astrophysique, Observatoire de Paris, Université Paris Diderot, CNRS, UPMC, Meudon, France.
[2]NASA Goddard Space Flight Center, Greenbelt, Maryland, USA.
[3]Southwest Research Institute, San Antonio, Texas, USA.

0094-8276/08/2008GL034912$05.00

1999a, 2001]. The analysis of the observed voltage power spectrum enables us to derive in situ several plasma parameters. In particular, it yields an accurate determination of the electron density N_e (accuracy of a few percent) since it is based on the location of the spectral peak just above the plasma frequency f_p, which is essentially independent of the receiver gain calibration. Moreover, the shape and level of the voltage spectrum provide accurate measurements of the core electron temperature in addition to other parameters.

3. Overview of the Third Fast Latitude Scan

[4] Figure 1 shows an overview of the radio observations during the Ulysses' third pole-to-pole passage. Figure 1 (top) displays the radio spectrogram (intensity coded by a color scale as a function of time and frequency) acquired by the Ulysses/URAP experiment during the fast latitude scan near the 2007 solar minimum. The intense fluctuating line is the plasma frequency f_p of the solar wind. One can see two distinct latitude regions as during the minimum of solar cycle 22 in 1994–1995 [*Issautier et al.*, 1998]: (1) a near-equatorial region, spanning around 30°S to 37°N in heliolatitude, where Ulysses crossed several times the heliospheric current sheet (HCS); (2) at higher latitudes, poleward of 30°S and 37°N, where Ulysses encountered for several months the stationary fast solar wind emanating from well developed polar coronal holes in both hemispheres. Compared to the first fast scan, the HCS extension is larger, more warped and slightly asymmetric, covering 30°S to 37°N in latitude. In this region, Ulysses alternatingly encountered slow and fast streams, shown by large variations of the plasma line. Figure 1 (bottom) shows the electron density and core temperature deduced from the QTN method (about 180,000 data points). Poleward of 30°S and 37°N, Ulysses measured the steady-state fast solar wind with a speed ranging from 700 to 800 km/s [*McComas et al.*, 2008]. In these high-latitude regions the plasma parameters are very steady (see Figures 2 and 3).

[5] Unfortunately, in contrast to the observations made during the first polar pass, the radial variations of these parameters obtained in polar coronal holes are severely limited due to spacecraft power shortage and sharing between instruments. Indeed, the URAP instrument was turned off until 1 May 2007, and definitively after 26 November 2007, to save and share energy onboard. So the highest heliolatitudes were inaccessible for the URAP data.

[6] Figure 2 shows the (1 AU scaled) electron density histograms (green) for both northern (about 64,400 measurements) and southern (about 63,000 measurements) hemispheres during the 2007 fast latitude scan. They are nearly gaussian, showing a single type of wind. We superimposed on them histograms obtained respectively in the northern and southern hemispheres during the first Ulysses polar pass (grey). In 2007, the mean scaled density of the fast wind from the northern polar coronal hole (37 to 68°N) is 2.06 cm^{-3} with a standard deviation of 0.62 cm^{-3}, being 16% less dense than during the last minimum in the northern polar coronal hole, from 40 to 80°N [*Issautier et al.*, 1998]. In the southern hemisphere (from 30 to 60°S), the mean scaled density of the fast wind is 2.09 cm^{-3} with a standard deviation of 0.58 cm^{-3}, being 21% less dense than during the last minimum in the southern polar coronal hole (40 to 80°S). Note that the standard deviation of the recent data is larger than during the first polar pass. In that latter case, the mean of the scaled density was 2.45 cm^{-3} with a standard deviation of 0.32 cm^{-3} in the northern hemisphere, and 2.65 cm^{-3} with a standard deviation of 0.4 cm^{-3} in the southern hemisphere [*Issautier et al.*, 1998]. Moreover, no significant asymmetry is observed between the northern and southern hemispheres during this third fast polar scan, in contrast to the first one, where the southern hemisphere was about 10% denser than the northern one. Note however that the 1994 south pass occurred slightly before activity minimum. It is noteworthy that the electron density is deduced from the plasma frequency cut-off to better than 5%.

[7] We now consider the electron core temperature T_c. We scale it non-adiabatically as $R^{-0.64}$ (R is the heliodistance of Ulysses in AU), which roughly matches most empirical determinations [*Issautier et al.*, 1999b] and theoretical expectations [*Meyer-Vernet and Issautier*, 1998]. Figure 3 shows the T_c histograms (orange) obtained from the northern (Figure 3, left) and southern (Figure 3, right) polar coronal holes during the 2007 fast latitude scan. We superimposed on each of these histograms the T_c distributions obtained during the previous solar minimum in the polar coronal hole wind of each hemisphere (grey). The distributions are nearly gaussian. In 2007, the northern fast wind has a mean scaled core temperature of 6.2×10^4 K with a standard deviation of 1.3×10^4 K, close to the (scaled) southern value of 6.43×10^4 K with a standard deviation of 1.1×10^4 K, implying no significant asymmetry between hemispheres. Note that the T_c histograms from the first fast latitude scan revealed a 10% asymmetry between northern and southern hemispheres, the latter being hotter. Note also that the 1994 south pass occurred slightly before activity minimum. The average of the scaled T_c is smaller than during the last solar minimum, showing a 11% (northern hemisphere) and 14% (southern hemisphere) difference respectively. During the first fast scan, the mean of the scaled core temperature was 7×10^4 K, with a standard deviation of 8.6×10^3 K in the northern hemisphere, and 7.5×10^4 K, with a standard deviation of 1.1×10^4 K, in the southern hemisphere [*Issautier et al.*, 1998]. Note that in 2007 the radial magnetic field scaled to 1 AU has dropped by more than 35% from 3.2 to 2.04 nT during the solar cycle in both hemispheres [*Smith and Balogh*, 2008], whereas the bulk solar wind speed was nearly similar to that obtained in 1994–1995, with a mean value of about 750 km/s [*McComas et al.*, 2008].

4. Comparison Over Solar Cycle and Discussion

[8] Figure 4 shows the electron flux normalised to 1 AU, $n_e V R_{AU}^2$ (dots) as a function of the heliolatitude, for the polar coronal hole wind observed during the three fast latitude scans, near the 1994–1995 and 2007 solar minima, and the 2001 solar maximum. We use the electron density n_e from the URAP experiment, and the solar wind speed V from the SWOOPS particle analyser [*Bame et al.*, 1992]. Note that for the 2007 minimum the electron flux plotted in triangles was deduced from the proton and alpha density measurements on the SWOOPS experiment, when the URAP instrument was turned off due to spacecraft power sharing at highest latitudes. Composite images from SOHO/EIT,

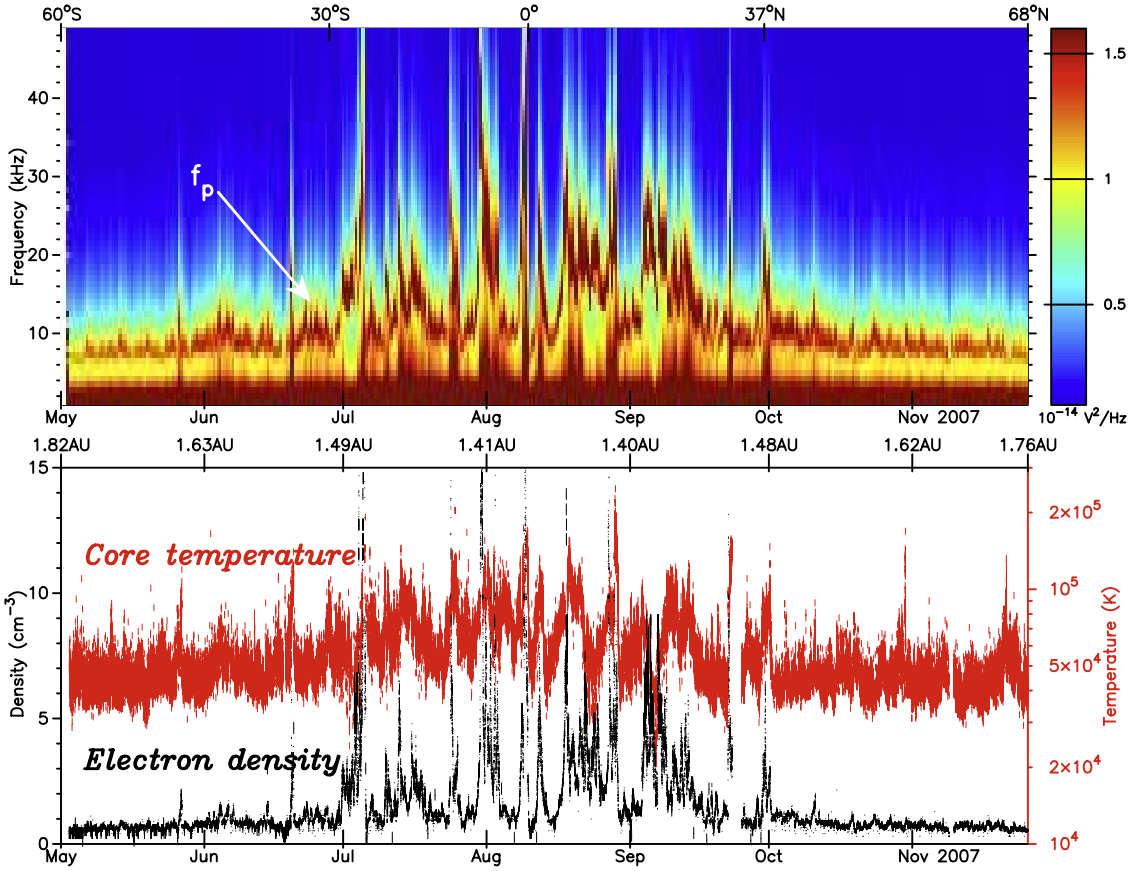

Figure 1. Radio spectrogram obtained from the URAP experiment during Ulysses' third fast latitude scan in 2007 at latitudes between 60°S and 68°N, with the corresponding electron density (black dots) and core temperature derived from QTN spectroscopy.

HAO Mauna Loa coronograph and SOHO/LASCO C2 show the corresponding state of the corona for these periods. In 1994–1995, the scaled electron flux (green symbols) in polar coronal holes is similar in both hemispheres at 1.9×10^{12} m^{-2} s^{-1} northward of 40°N, and 2×10^{12} m^{-2} s^{-1} southward of 40°S. The blue dot is the scaled electron flux in the northern polar coronal hole during the fast latitude scan at the 2001 solar maximum. The flux is 2.1×10^{12} m^{-2} s^{-1}, roughly equal to those of 1994–1995, showing similar flux from polar coronal holes at the solar minimum and maxi-

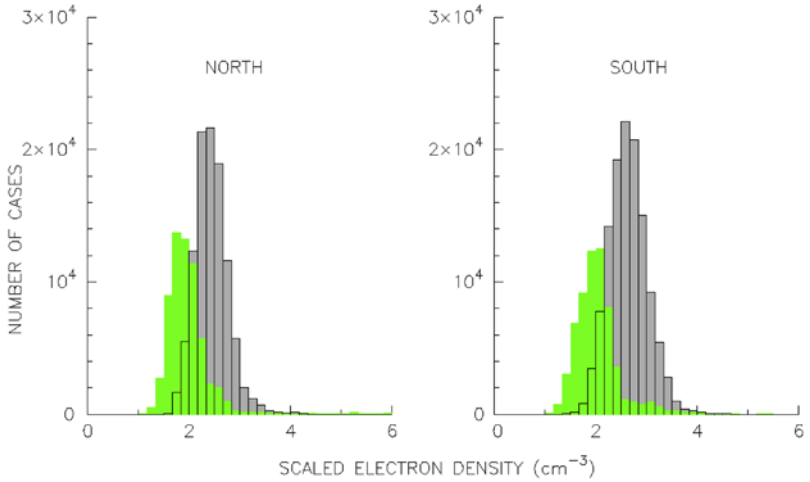

Figure 2. Histograms of electron density scaled to 1 AU, with a bin size of 0.17, near the 2007 solar minimum during Ulysses' third fast latitude scan (green), (left) northward of 37° and (right) southward of 30°. Grey histograms correspond to the scaled electron density obtained during Ulysses' first latitude scan poleward of 40° for both hemispheres.

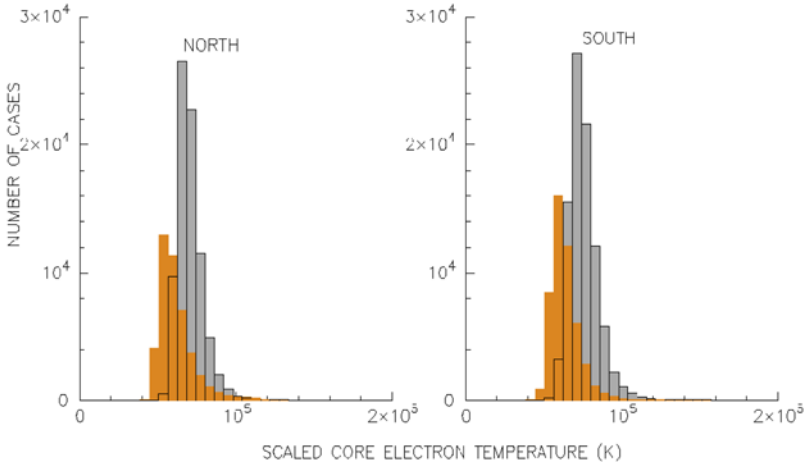

Figure 3. Histograms of electron core temperature scaled to 1 AU assuming a $R^{-0.64}$ variation, with a bin size of 5×10^3, near the 2007 solar minimum during Ulysses' third fast latitude scan (orange), (left) northward of 37° and (right) southward of 30°. Grey histograms are the scaled core temperature obtained during Ulysses' first latitude scan poleward of 40° for both hemispheres.

mum. In contrast, the fast polar pass in 2007 exhibits a large drop in the average scaled electron flux, both in the northern (orange) at 1.4×10^{12} m^{-2} s^{-1} and southern hemispheres (red) at 1.5×10^{12} m^{-2} s^{-1}. This corresponds to a drop of about 25% in particle flux between the 1994–1995 and 2007 solar minima. In both minima, the mean is almost constant with heliolatitude in each hemisphere, namely the product of the flux by the distance squared is nearly independent of latitude.

[9] What is the origin of the drop in density and temperature between the minima of solar cycles 22 and 23? In fact, the fast latitude scan during cycle 22 took place slightly before the minimum, so that the average sunspot number was somewhat smaller during the 2007 fast latitude scan than in 1994–1995. One should then expect a smaller HCS

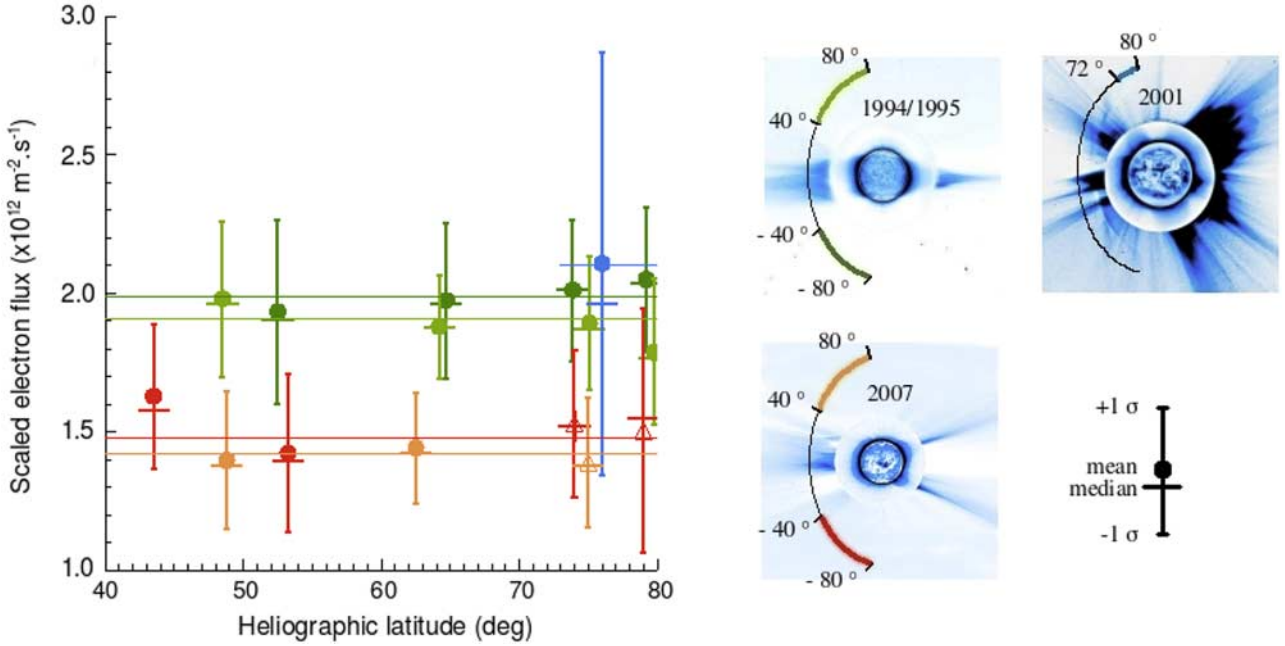

Figure 4. (left) Scaled electron flux versus the modulus of the heliographic latitude in polar coronal hole wind during the Ulysses fast latitude scans shown (right) near minimum in 1994–1995 (green for north pole and dark green for south pole), near maximum in 2001 (blue dot for northern coronal hole), and near minimum in 2007 (orange for north pole and red for south pole). Measurements are binned over a solar rotation and displayed with the corresponding mean and median. The average over latitude of the scaled electron flux in the fast wind for both minima is shown by horizontal lines, each color corresponding to each hemisphere. Also shown is composite of EIT (center), HAO Mauna Loa coronograph (inner ring) and LASCO C2 (outer ring) coronal images during the three periods of Ulysses' fast latitude scan labeled in the figure.

tilt and extension in 2007. Instead, as seen in Figure 1 from the electron measurements, the HCS has a larger extension. This may be due to the fact that in 2007 polar coronal holes are not as well developed as in 1994–1995; furthermore, the STEREO mission observed a mid-latitude coronal hole, which is unexpected at solar minimum, suggesting a complex solar magnetic field. Indeed, the composite coronal image of SoHo shown in Figure 4 during the 2007 fast latitude scan, has an unusual coronal structure for a solar minimum configuration.

[10] Be that as it may, variations from cycle to cycle in polar corona and solar wind properties are not unusual. For example, the interplanetary magnetic field was lower than average in cycle 20 [*Richardson et al.*, 2002]. A secular increase in the area of polar zones at activity minimum with a corresponding decrease in coronal temperature at high latitudes has been suggested [*Makarov et al.*, 2004]. Finally, the variations observed in the solar wind properties might be related to the 22 year cycle or longer period ones, due to fluctuations of the solar dynamo [see, e.g., *Weiss*, 1994].

[11] **Acknowledgments.** The Ulysses URAP investigation is a collaboration of NASA/GSFC, Observatoire de Paris, University of Minnesota, and CETP, Velizy, France. The French contribution is supported by CNES and CNRS. We thank the SOHO/EIT instrument team, the SOHO/LASCO instrument team and the High Altitude Mauna Loa coronograph team for providing composite solar images of Figure 4.

References

Bame, S. J., et al. (1992), Ulysses solar wind plasma experiment, *Astron. Astrophys. Suppl. Ser.*, *92*(2), 237.

Issautier, K., N. Meyer-Vernet, M. Moncuquet, and S. Hoang (1998), Solar wind radial and latitudinal structure: Electron density and core temperature from Ulysses thermal noise spectroscopy, *J. Geophys. Res.*, *103*, 1969–1979.

Issautier, K., N. Meyer-Vernet, M. Moncuquet, S. Hoang, and D. McComas (1999a), Quasi-thermal noise in a drifting plasma: Theory and application to solar wind diagnostic on Ulysses, *J. Geophys. Res.*, *104*, 6691–6704.

Issautier, K., N. Meyer-Vernet, M. Moncuquet, and S. Hoang (1999b), High-speed solar wind from Ulysses measurements and comparison with exospheric models, in *Proceedings of the Ninth International Solar Wind Conference*, edited by S. R. Habbal et al., *AIP Conf. Proc.*, *471*, 581–585.

Issautier, K., R. M. Skoug, J. T. Gosling, S. P. Gary, and D. J. McComas (2001), Solar wind plasma parameters on Ulysses: Detailed comparison between the URAP and SWOOPS experiments, *J. Geophys. Res.*, *106*, 15,665–15,675.

Issautier, K., et al. (2003), Large-scale structure of the polar solar wind at solar maximum: Ulysses/URAP observations, in *10th International Conference on Solar Wind*, edited by M. Velli, *AIP Conf. Proc.*, *679*, 263–266.

Issautier, K., M. Moncuquet, and S. Hoang (2004), Solar wind electron parameters from Ulysses/URAP quasi-thermal noise measurements at solar maximum, *Sol. Phys.*, *221*, 351–360.

Luhmann, J. G., et al. (2002), Solar cycle changes in coronal holes and space weather cycles, *J. Geophys. Res.*, *107*(A8), 1154, doi:10.1029/2001JA007550.

Makarov, V. I., A. G. Tlatov, and D. K. Callebaut (2004), Long-term changes of polar activity of the Sun, *Sol. Phys.*, *224*, 49–59.

McComas, D. J., et al. (2000), Solar wind observations over Ulysses' first full polar orbit, *J. Geophys. Res.*, *105*, 10,419–10,433.

McComas, D. J., et al. (2002), Ulysses' second fast-latitude scan: Complexity near solar maximum and the reformation of polar coronal holes, *Geophys. Res. Lett.*, *29*(9), 1290, doi:10.1029/2001GL014164.

McComas, D. J., et al. (2003), The three-dimensional solar wind around solar maximum, *Geophys. Res. Lett.*, *30*(10), 1517, doi:10.1029/2003GL017136.

McComas, D. J., et al. (2008), Weaker solar wind from the polar coronal holes and the whole Sun, *Geophys. Res. Lett.*, doi:10.1029/2008GL034896, in press.

Meyer-Vernet, N., and K. Issautier (1998), Electron temperature in the solar wind: Generic radial variation from kinetic collisionless models, *J. Geophys. Res.*, *103*, 29,705–29,717.

Meyer-Vernet, N., et al. (1998), Measuring plasma parameters with thermal noise spectroscopy, in *Measurement Techniques in Space Plasmas: Fields*, *Geophys. Monograph Ser.*, vol. 103, edited by R. Pfaff et al., pp. 205–210, AGU, Washington, D. C.

Neugebauer, M. (2001), The solar wind and heliospheric magnetic field in three dimensions, in *The Heliosphere Near Solar Minimum: The Ulysses Perspective*, edited by A. Balogh, R. Marsden, and E. J. Smith, pp. 43–99, Springer, New York.

Phillips, J., et al. (1995), Ulysses solar wind plasma observations from pole to pole, *Geophys. Res. Lett.*, *22*, 3301–3304.

Richardson, I. G., E. W. Cliver, and H. V. Cane (2002), Long-term trends in interplanetary magnetic field strength and solar wind structure during the twentieth century, *J. Geophys. Res.*, *107*(A10), 1304, doi:10.1029/2001JA000507.

Smith, E. J., and A. Balogh (2008), Decrease in heliospheric magnetic flux in this solar minimum: Recent Ulysses magnetic field observations, *Geophys. Res. Lett.*, doi:10.1029/2008GL035345, in press.

Smith, E. J., et al. (2003), The Sun and the heliosphere at solar maximum, *Science*, *302*, 1165–1169.

Stone, R. G., et al. (1992), The unified radio and plasma wave investigation on Ulysses, *Astron. Astrophys. Suppl.*, *92*, 291.

von Steiger, R., et al. (2001), The 3-D heliosphere from the Ulysses and ACE Solar Wind Ion Composition experiments, *Space Sci. Rev.*, *97*, 123–127.

Weiss, N. O. (1994), Solar and stellar dynamos, in *Lectures on Solar and Planetary Dynamos*, edited by M. R. E. Proctor and A. D. Gilbert, pp. 59–95, Cambridge Univ. Press, New York.

S. Hoang, K. Issautier, G. Le Chat, N. Meyer-Vernet, and M. Moncuquet, Laboratoire d'Etudes Spatiales et d'Instrumentation en Astrophysique, Observatoire de Paris, Université Paris Diderot, CNRS, UPMC, 5 place Jules Janssen, F-92195 Meudon CEDEX, France. (karine.issautier@obspm.fr)

R. J. MacDowall, NASA Goddard Space Flight Center, Code 695, Greenbelt, MD 20771, USA.

D. J. McComas, Southwest Research Institute, P.O. Drawer 28510, San Antonio, TX 78228-0510, USA.